Received: December 24, 2021. Revised: March 7, 2022. 242

International Journal of
Intelligent Engineering & Systems

http://www.inass.org/

Adaptive Grasshopper Optimization Algorithm for Multi-Objective Dynamic Optimal Power Flow in Renewable Energy Integrated Microgrid

P. Sobha Rani[1]* M. S. Giridhar[1] K. Radha Rani[2] Varaprasad Janamala[3]

[1]*Lakireddy Bali Reddy College of Engineering (Autonomous), Jawaharlal Nehru Technological University Kakinada (JNTUK), Kakinada, East Godavari, Andhra Pradesh, India*
[2]*R.V.R & J.C. College of Engineering, Chowdavaram, Guntur, Andhra Pradesh, India*
[3]*School of Engineering and Technology, CHRIST (Deemed to be University), Bangalore, Karnataka, India*
* Corresponding author's Email: sobhareveru@gmail.com

Abstract: Global warming has prompted several governments to adopt more sustainable policies in all areas. Incorporating renewable energy sources (RES) and adopting electric vehicles (EVs) are examples of such practises. Today's electrical distribution networks (EDNs) are becoming more reliable microgrids (MG) that can operate grid-connected or self-healing. As a result, the fluctuating nature of RES and EVs has raised numerous technical and economic concerns. This research proposes a novel multi-objective dynamic optimum power flow (OPF) addressing total load dispatch cost minimization and network security margin maximisation for various load profiles. A composite load model is proposed considering residential, industrial, commercial, EVs, agricultural loads. The proposed optimization issue is tackled using an adaptive grasshopper optimization algorithm (AGOA), a meta-heuristic grasshopper optimization technique with adaptive control parameter (AGOA). A modified IEEE 33-bus benchmark test system with PV units and reactive power compensation devices is used for simulation over 24-hour horizon. The suggested AGOA's computing efficiency is compared for two scenarios. By combining good exploration and exploitation features with adaptive regulating variables, the AGOA outperformed in terms of global optima. Also, the techno-economics of MG operation and control are improved significantly. In scenario 1, the network is configured in a radial topology, with average operational costs, distribution losses, voltage variation, and transmission loadability of 1117.72 $/h, 82.4803 kW, 0.0058 p.u., and 0.7910 p.u., respectively, over a 24-hour period. In scenario 2, the network is run as a meshed network, with network performance of 1113.36 $/h, 43.15 kW, 0.0019 p.u., and 0.8524 p.u., respectively. This suggests that switching from radial to meshed configuration can result in lower losses, a better voltage profile, and increased loadability, as well as the applicability of the suggested methodology for managing uncertainty in modern EDNs.

Keywords: Optimal power flow, Adaptive grasshopper optimization, Photovoltaic generation, Composite load modelling, Enhanced IEEE 33-bus benchmark test system.

1. Introduction

Traditionally, the preventive and corrective measures for ensuring the secure and reliable operation in power systems are highly in conflict with economic goals and environmental aspects. On the other side, the planning and decision-making stages need to develop for economic goals as well as currently inclined towards environmental aspects concerning global warming across the world. In order to surpass these barriers, optimization becomes one of the essential tools in modern power system operation and control.

In a general framework for economic operation, unit commitment (UC), economic load dispatch (ELD) and optimal power flow (OPF) are more popular and major optimization problems [1]. Most importantly, these three problems are also related to each other in a complicated way. In an UC problem, the solution aims to determine least cost scheduling of generating units to meet timely varying load patterns considering spinning reserve (SR)

requirements [2]. In recent times, minimization of greenhouse gas (GHG) emission has also become one of the major objective functions in the UC problem with various operational constraints such as power demand, spinning reserve, generation real and reactive power limits, ramping rate limits and minimum up and down time limits etc [3].

The solution of the ELD problem aims to minimize the operating cost of running generating units, which are scheduled at the UC problem stage by determining real power outputs for a specific load demand. Predefined transmission losses are also handled in this problem. The generators' minimum and maximum generation limits for real power are the key constraints in this problem [4].

On the other hand, OPF problem is an extension of ELD problem considering dispatchable constraints of the transmission system [5]. In order to achieve techno-economic efficient operation, congestion management (CM) approaches become inevitable in transmission system power flow control. Particularly, integration of FACTS optimally becomes a prominent and an efficient solution among all CM approaches [6]. In specific, generation cost, transmission loss, voltage stability, transmission loadability, congestion relief and voltage profile etc., are some of the major objective functions that have been considered in this optimization problem. Coming to operational constraints, power demand, real and reactive power generation limits, minimum up and down time limits, lime MVA limits, bus voltage magnitude and their angle limits, shunt VAr injection limits, tap-changer limits etc., are handled.

On the other hand, in techno-economic-environmental framework, integration of distribution generation (DGs), renewable energy sources (RES) and demand side management (DSM) are becoming efficient solutions in the modern distribution networks and transforming towards more reliable microgrids [7, 8], particularly at the distribution side. At this stage, it is essential to realize the complexity of optimization in almost all stages of the power system (including generation, transmission and distribution) considering multiple objective functions and operational constraints. In literature various optimization approaches have been adopted so far for solving these problems either sequentially or simultaneously [9]. However, heuristic approaches have been identified highly in recent times due to their various advantages than conventional approaches [10]. In [11], whale optimization algorithm (WOA) with wavelet mutation is proposed for OPF by handling simultaneous minimization of power loss and voltage deviation under multi-objective function. In [12], multi-objective ant lion algorithm (MOALO) with fuel cost, emission, losses and voltage profile is handled while solving OPF problem. In [13], multi-verse optimization (MVO), (GOA), and harris hawks optimization (HHO) are adapted for OPF problem with fuel cost and losses. In [14], cuckoo search algorithm (CSA) and sunflower optimization (SFO) and their hybrid approach (HCSA-SFO) is developed for OPF problem. In [15], non-dominated sorting genetic algorithm-2 (NSGA-II) is introduced for cost and voltage deviation minimization in OPF problem considering voltage-dependent load modelling. Similarly, forced initialized multi-objective differential evolution algorithm (MODEA) [16], particle swarm optimization (PSO)-gravitational search algorithm (PSO-GSA) [17], differential evolution (DE) [18], backtracking search algorithm (BSA) for loss, emission and voltage deviation minimization [19], moth flam optimizer (MFO) [20], improved colliding bodies optimization (ICBO) [21] and improved chaotic electromagnetic field optimization (ICEFO) [22] etc are some such recent works for OPF problem.

However, no single algorithm is capable and suitable for all kinds of optimization problems [23]. This fact becomes another motivation for selecting an efficient meta-heuristic grasshopper optimization algorithm (GOA) in this work [24]. In recent times, GOA has attained high attention for solving different kinds of optimization problems [25, 26]. However, the basic GOA suffers with local optima with less exploration capabilities. To overcome this, linearly decreasing adaptive factor c is proposed for balancing exploration and exploitation phases in AGOA [27].

On the other hand, considering renewable energy sources and their variability, OPF problem is handled in few works. DE [28] and grey wolf optimizer (GWO) [29] are proposed for handling the stochastic nature of solar power plants in OPF problem. In [30], sunflower optimization algorithm (SOA) is proposed for dealing OPF considering variability in PV and wind turbine (WT) power units. In [31], dragonfly algorithm (DA) with ageing PSO (DA-PSO) is developed for OPF with WT power variation. In [32], PV variability is handled in security constrained OPF along with simultaneous control of optimal unified power flow controller (OUPFC) under (N-1) line contingencies.

From these works, it can be seen that the OPF problem is efficiently handled by using heuristic approaches. But all these works are focused on OPF problem in power transmission system considering constant power load. But in recent times, the modern

EDNs are becoming more active networks by the integration of various renewable energy based distributed generation (DG) units and self-healing capable microgrids (MG). In this aspect, OPF problem considering MG environment along with variability in RES and different kinds of load profiles (such as residential, industrial, commercial, agricultural and electric vehicle loads, etc) is not handled so far. Thus, this work is the first such kind of research focusing OPF problem in MGs with variability. In addition, various new meta-heuristics have been developed for solving different real-time complex optimization problems. The Mayfly algorithm is a recent and efficient algorithm, and it was proposed for the first time to solve this type of multi-variable multi-optimization problem in electrical engineering. The simulation studies are performed on modified IEEE 33-bus benchmark test system [33].

The remainder of the paper is laid out as follows: The mathematical modelling of major components in a modified IEEE 33-bus microgrid is described in section 2. The proposed multi-objective OPF problem with different operational constraints is presented in section 3. The notion of Mayfly optimization and its solution approach are presented in section 4. The results achieved using MOA are detailed in section 5, and the major contribution of this research is summarised in section 6.

2. Modelling of modified IEEE 33-bus microgrid components

In our work, the modified IEEE 33-bus benchmark test system [33] is considered as grid-connected MG, which has photovoltaic generation units, different kinds of loads such as residential, industrial, commercial and agricultural and electric vehicle loads are considered. Also, dynamic reactive power compensators like switched capacitor bank (SCB)/ D-STATCOMs are considered. According to Newton-Raphson (NR) load flow theory, the buses with PV units are chosen as generator buses/PV buses, the buses with reactive power compensation are considered as voltage-controlled buses, and the sub-station bus is treated as slack bus. And all other buses are treated as load buses/PQ buses. In addition, the network can be transformed to loop network from radial configuration by considering three tie-lines. In this section, the variability in PV power and network loading profile considering different types of loads are presented here.

2.1 Modeling of photovoltaic generation

Considering a PV unit of maximum capacity at bus-*k*, the net effective loading profile is modeled as,

$$P_{dk(t)}^{net} = \gamma_{k(t)} P_{dk}^{base} - P_{gk(t)} \tag{1}$$

$$P_{gk(t)} = P_{PV,k}^{max} \frac{G_{(t)}}{G_{ref}} \tag{2}$$

where $P_{dk(t)}^{net}$ and P_{dk}^{base} are the net effective load at bus-*k* after compensating PV generation and base case connected load, respectively; P_{gk} is the real power generation at bus-*k*, $\gamma_{k(t)}$ is a scaling factor between [0,1] for defining variability in load at bus-*k*, $P_{PV,k}^{max}$ is the maximum installed PV unit capacity, $G_{(t)}$ and G_{ref} are the radiation at time-t and reference radiation at STC, respectively.

2.2 Modeling of network load profile

In general, EDNs serve different kinds of loads such as residential (RL), industrial (IL), commercial (CL), transportation/ electric vehicles (EVL), and agriculture (AL), etc, which may have different daily load profile. However, the power consumption of any kind load is dependent on its associated bus voltage magnitude as defined in voltage-dependent load modelling [34]. Here, a composite load model is proposed by considering aforementioned loads and given by,

$$P_{dk(t)}^{net} = P_{dk}^{ref} \begin{Bmatrix} \gamma_{r(t)} A^{\alpha_r} + \gamma_{i(t)} A^{\alpha_i} + \\ \gamma_{c(t)} A^{\alpha_c} + + \gamma_{e(t)} A^{\alpha_e} \\ + \gamma_{a(t)} A^{\alpha_a} \end{Bmatrix} \tag{3}$$

$$Q_{dk(t)}^{net} = Q_{dk}^{ref} \begin{Bmatrix} \gamma_{r(t)} A^{\beta_r} + \gamma_{i(t)} A^{\beta_i} + \\ \gamma_{c(t)} A^{\beta_c} + + \gamma_{e(t)} A^{\beta_e} \\ + \gamma_{a(t)} A^{\beta_a} \end{Bmatrix} \tag{4}$$

where $A = |V_{k(t)}|/|V_{ref}|$, $|V_{k(t)}|$ and $|V_{ref}|$ are the actual and nominal voltage magnitudes of bus-*i*, respectively; $P_{dk(t)}^{net}$ and $Q_{dk(t)}^{net}$ are the net real and reactive power loads of bus-*i* respectively; P_{dk}^{ref} and Q_{dk}^{ref} are the real and reactive power loads of bus-*i* at nominal voltage, respectively; $(\gamma_{r(t)}, \alpha_r, \beta_r)$, $(\gamma_{i(t)}, \alpha_i, \beta_i)$, $(\gamma_{c(t)}, \alpha_c, \beta_c)$, $(\gamma_{e(t)}, \alpha_e, \beta_e)$ and $(\gamma_{a(t)}, \alpha_a, \beta_a)$ are the (fraction of load, real power exponent and reactive power exponents) for residential, industrial, commercial, electric vehicles and agricultural type of loads, respectively.

3. Problem formulation

In order to ensure secure and reliable power supply, various operational constraints need to be satisfied at each section in the power system. Hence, considering security, reliability and dispatchable problems to the generation schedule derived at ELD stage, the optimal power flow (OPF) problem can be formulated as a multi-objective optimization problem.

3.1 Objective functions

Operating cost minimization, loss minimization, voltage profile enhancement and transmission system loadability enhancement etc, are the major objective functions used to define multi-objective function, as in Eq. (5),

$$OF = f_1 + f_2 + f_3 + f_4 \quad (5)$$

3.1.1. Operating cost

The fundamental objective of OPF is to minimize the cost of real power production without compromising operational constraints. The production can be obtained by using cost curves of generating units and expressed as in Eq. (6) for first objective function $f_1 = C_{(t)}$.

$$f_1 = \sum_{k=1}^{N_g} \left(a_k P_{gk}^2 + b_k P_{gk} + c_k\right) \$/h \quad (6)$$

where N_g is the number of generators, P_{gk} is the real power generation at bus-k, a_k, b_k and c_k are the coefficients for determining fuel cost of a generator.

3.1.2. Distribution loss

Minimization of transmission/distribution losses can relieve the burden on generation units and consequently, results for low production cost and efficient system operation. The total real power losses can be determined by summing losses of all lines in the system, as given in Eq. (7) for second objective function $f_2 = P_{loss(t)}$.

$$f_2 = \sum_{\substack{k=1 \\ \in(p,q)}}^{N_{br}} g_k\left(V_p^2 + V_q^2 - 2V_pV_q cos\theta_{pq}\right) kW \quad (7)$$

where N_{br} is the number of branches in the network, k-is the branch index connected between buses p and q, V_p and V_q are the voltage magnitudes of bus-p and bus-q, respectively, g_k is the conductance of branch-k, θ_{pq} is the load angle difference between bus-p and bus-q.

3.1.3. Voltage profile

Voltage profile: In power systems, low voltage profiles may cause high current flows in transmission lines and consequently more losses may take place. In addition, it also leads to voltage instability and hence, managing adequate voltage profile is an important task. Considering maximum bus voltage magnitude as reference, the average voltage deviation index (AVDI) is defined for third objective $f_3 = AVDI_{(t)}$ as given in Eq. (8). Minimization of this index ensures a good voltage profile across the network.

$$f_3 = \frac{1}{N_b}\sum_{k=1}^{N_b}\sqrt{\left(|V_{ref}| - |V_{k(t)}|\right)^2} \quad (8)$$

where N_b is the number of buses in the network.

3.1.4. Transmission system loadability

In order to avoid high generation cost due to congestion and to ensure secure power flows, the transmission lines should not be overloaded for any schedule at any time. Hence, maximization of transmission security margin (TSM) defined in Eq. (9) as objective $f_4 = TSM_{(t)}$,

$$f_4 = \frac{1}{N_{br}}\sum_{\substack{k=1 \\ \in(p,q)}}^{N_{br}}\left(1 - \frac{S_{k(p,q)} + S_{k(q,p)}}{2S_k^{max}}\right) \quad (9)$$

where S_k and S_k^{max} are the apparent power flow of branch-k connected between buses p and q, and its maximum power flow limit. TSM should be near to 1 for having high security margin for a given schedule.

3.2 Operating constraints

Power flow equations corresponding to both real and reactive power balance equations are the equality constraints that should satisfy at every scheduling hour-t, as given in Eqs. (10) and (11), respectively.

$$\sum_{k=1}^{N_g} P_{gk(t)} + P_{grid(t)} = P_{loss(t)} + \sum_{k=1}^{N_b} P_{dk(t)}^{net} \quad (10)$$

$$\sum_{k=1}^{N_{bc}} Q_{ck} + Q_{grid(t)} = Q_{loss(t)} + \sum_{k=1}^{N_b} Q_{dk(t)}^{net} \quad (11)$$

The real power generation limits$\left(P_g\right)$, reactive power generation limits$\left(Q_g\right)$, voltage magnitude limits $|V_k|$, phase angle limits δ, tap-changing transformer control limits a_t, shunt MVAr injection limits Q_c and line MVA limits S_k, are the major

unequal constraints in OPF problem and defined in Eqs. (12)-(18), respectively.

$$P_{gk}^{min} \le P_{gk(t)} \le P_{gk}^{max}, \forall k = 1{:}\, N_g \quad (12)$$

$$Q_{gk}^{min} \le Q_{gk(t)} \le Q_{gk}^{max}, \forall k = 1{:}\, N_g \quad (13)$$

$$\left|V_k^{min}\right| \le \left|V_{k(t)}\right| \le |V_k^{max}|, \forall k = 1{:}\, N_b \quad (14)$$

$$\delta_k^{min} \le \delta_{k(t)} \le \delta_k^{max}, \forall k = 1{:}\, N_b \quad (15)$$

$$a_t^{min} \le a_{t(t)} \le a_t^{max}, \forall k = 1{:}\, N_t \quad (16)$$

$$Q_{ck}^{min} \le Q_{ck} \le Q_{ck}^{max}, \forall k = 1{:}\, N_{nc} \quad (17)$$

$$max\left(\left|S_{k(p,q)}\right|, \left|S_{k(q,p)}\right|\right) \le S_k^{max}, \forall k = 1{:}\, N_{br} \quad (18)$$

where N_t and N_{nc} are the number of tap-changers and number of shunt VAr compensation locations.

As seen in the mathematical model for OPF problem, various parameters and controlling variables are needed to optimize simultaneously. The reactive power generations are interdependent on generator bus voltage magnitudes. The real power generations including transmission losses are interdependent on current flows and subsequently on load bus voltage magnitudes, phase angles and admittances, tap-ratios, shunt MVAr injections etc. Hence, calculation of bus voltage magnitudes and phase angles w.r.t. real and reactive power injections and all other controlling parameters, is very important in OPF problems. Generally, Newton-Raphson (NR) load flow technique is a very powerful tool for solving nonlinear load flow equations.

4. Proposed solution methodology

Here, the proposed solution methodology using adaptive grasshopper optimization algorithm (AGOA) and implementation procedure while solving OPF problem is discussed mathematically.

4.1 Adaptive grasshopper optimization

By nature, grasshoppers are insects, due to their damage to the crop and agriculture treated as pets. Also, they are usually seen individually but can join and form the largest swarm, which may become a nightmare for farmers. The grasshopper swarms during nymph/larval phase jump and moves like a cylinder. During this phase, their movement is slow and in small steps. On the other side, adulthood phase grasshopper swarms can be able to migrate from one continent to another by flying in air itself. At this phase, the movement is abrupt and long range. In both the phases, they seek food and eat all vegetarian in their swarming path. This specific swarming nature is the basic motivation for the introduction of the grasshopper optimization algorithm (GOA) by Mirjalili S in 2016 [24].

As known in any nature-inspired optimization algorithm, the search process has two stages i.e., exploration and exploitation. The abrupt and long-range swarming nature of the adult phase is handled in exploitation and the slow and small-step swarming nature of larval phase is handled in the exploitation stage. These two stages with food targets are modelled in the simulation behaviour of grasshoppers. The mathematical model employed in GOA is as follows.

The position of *k*th grasshopper X_k is depends on social influence S_k, gravity force G_k and wind advection A_k.

$$X_k = S_k + G_k + A_k \quad (19)$$

In order to provide random nature, three uniformly distributed random numbers r_i are introduced to Eq. (19) and given in Eq. (20).

$$X_k = r_1 S_k + r_2 G_k + r_3 A_k \quad (20)$$

The social influence factor is modelled as a function (s) with strength of social forces by considering the distance between *k*th and *i*th positioned grasshoppers $(\overline{d_{ik}})$ and a directional unit vector $(\overline{a_{ik}})$ as given in Eq. (21).

$$S_k = \sum_{\substack{i=1 \\ \neq k}}^{N} S\left(\overline{d_{ik}}\right)\overline{a_{ik}} \quad (21)$$

where $\overline{d_{ik}} = x_i - x_k$ and $\overline{a_{ik}} = \frac{\overline{d_{ik}}}{|\overline{d_{ik}}|}$ and N is the number of grasshoppers.

The social force function s is determined using Eq. (22),

$$s(r) = f e^{\frac{-r}{l}} - e^{-r} \quad (22)$$

where *f* is the intensity of attraction and *l* is the scale of attractive length. The social force can be either attraction or repulsion. By changing *f* and *l*, different social forces can be formulated.

Similarly, gravity force G_k and wind advection A_k components are calculated as given in Eq. (23).

$$G_k = -g\bar{e}_g \text{ and } A_k = u\bar{e}_w \quad (23)$$

where g and u are the gravitational and drift velocity constants respectively; $\bar{e}_g$ and $\bar{e}_w$ are the unit vectors towards the centre of earth and in the direction of wind respectively.

The expanded version of Eq. (20) by substituting Eq. (21) to Eq. (23) can be written as Eq. (24).

$$X_k = \sum_{\substack{i=1 \\ \neq k}}^{N} S(\overline{d_{ik}})\overline{a_{ik}} - g\bar{e}_g + u\bar{e}_w \quad (24)$$

However, the swarming behaviour of grasshoppers expressed in Eq. (24) may not suit directly to solve optimization problems, since grasshoppers quickly reach their comfort zone and do not converge to precise points. In order to overcome this, Eq. (24) is slightly modified as given in Eq. (25).

$$X_k^d = c\left\{\sum_{\substack{i=1 \\ \neq k}}^{N}\left(\frac{ub_d - lb_d}{2}\right)S(\overline{d_{ik}})\overline{a_{ik}}\right\} + \overline{T_d} \quad (25)$$

where ub_d and lb_d are the upper and lower limits in the Dth dimension respectively; $\overline{T_d}$ is the best solution found so far for the value of target in the Dth dimension and c is the adaptive parameter or decreasing inertia coefficient to shrink the comfort, repulsion and attraction zones, which is given in Eq. (26).

$$c = (c_{max} - 1)\left\{\frac{it(c_{max} - c_{min})}{it_{max}}\right\} \quad (26)$$

In order to maximize local search ability, enhance accuracy and for low computational time, improved inertia weight is introduced in adaptive GOA (AGOA) [27] and it is given in Eq. (27),

$$c = c_{max} - (c_{max} - c_{min})(it/it_{max})^{1/it} \quad (27)$$

where it_{max} is the number of maximum iterations and the minimum and maximum value of c are $c_{min} = 0.00001$ and $c_{max} = 1$.

4.2 AGOA for OPF Problem in MG

The steps involved in solving OPF problem in MG considering SPV generation and load variability are presented in Fig. 1.

In each scheduling hour, the maximum real power limit at PV buses is adjusted to power generation of SPV units subjected to solar radiation at that time. Also, the net load of each bus is adjusted at each hour in accordance to the variability in each kind of load.

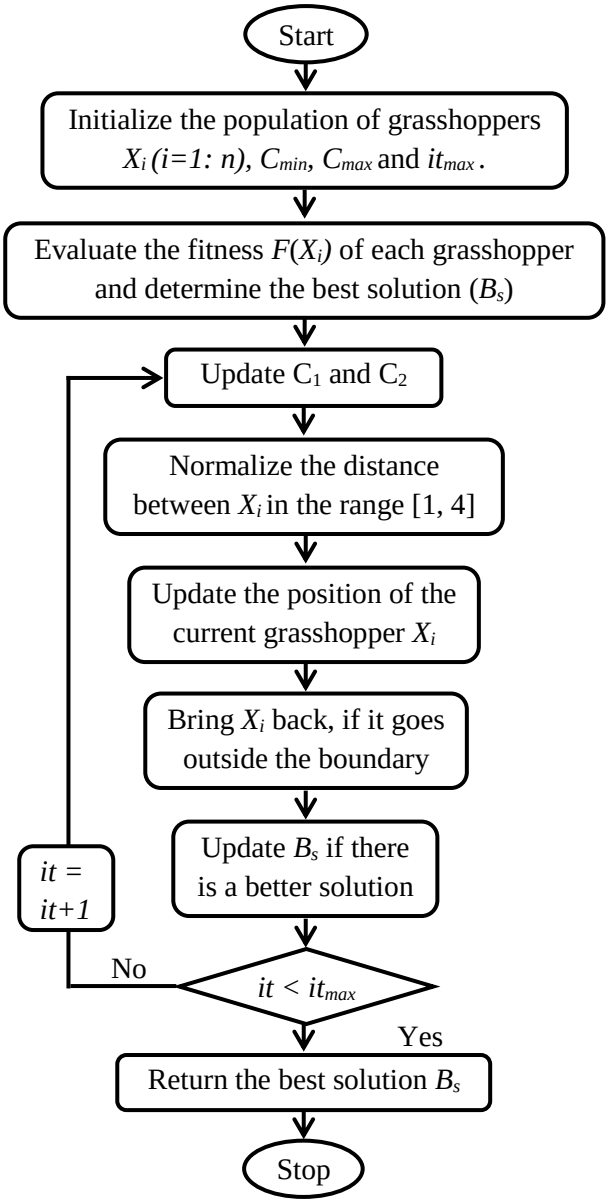

Figure. 1 Flowchart of the AGOA for OPF problem

5. Simulation results

Simulations are performed for two scenarios. In Scenario 1, the computational efficiency of AGOA is validated by solving OPF problem in microgrid consisting of PV uncertainty, and different types of loads. In Scenario 2, AGOA is implemented for OPF problem in conventional power system and compared with literature.

5.1 OPF Problem in microgrid

As described in section 2, the modified IEEE 33-bus benchmark test system [33] is considered as grid-associated MG integrated with four SPV type

DGs at bus-18, 22, 25 and 33, of maximum capacities of 200 kWp. These buses are treated as PV buses. Also, two D-STATCOMs at bus-18 and 33 are integrated in sizes of 400 kVAr and 600 kVAr, respectively. Thus, the maximum reactive power generation limits at bus-18 and 33 are set to D-STATCOM capacities, whereas for bus-22 and 25, both minimum and maximum reactive power limits are set to zero. On the other hand, the output power from SPVs is estimated using PVWatts® calculator [36] by considering Bangalore weather conditions (Lat, Lon: 12.95^0, 77.55^0) and set as maximum real power generation limit for each scheduling hour. The maximum power generation is noticed on February 22, 2022 at 12:00pm as 154.367 kW and correspondingly, the typical daily output curve is given in Fig. 2.

The details of cost coefficients for DGs and grid supply, the constant power loads at each bus and also the branch data are taken from [33]. In the proposed composite load model, 30 % residential, 25 % industrial, 20 % commercial, 10 % EV, and 15 % agricultural load shares are considered at each bus. In order to maintain simple calculations, $\gamma_{k(t)}$ is considered same for all types of loads and set equal to same as hourly load profile defined in [33] and is given in Fig. 3.

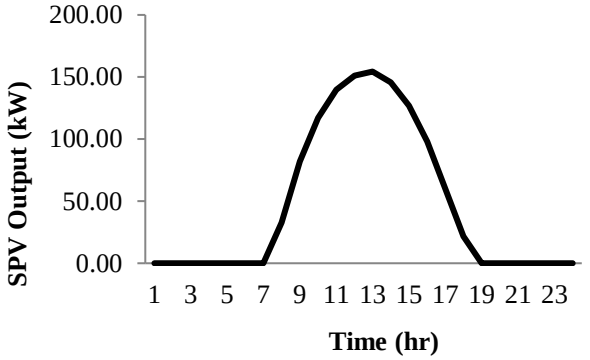

Figure. 2 Typical daily generation curve of a 200 kWp SPV unit as estimated on February 22, 2022

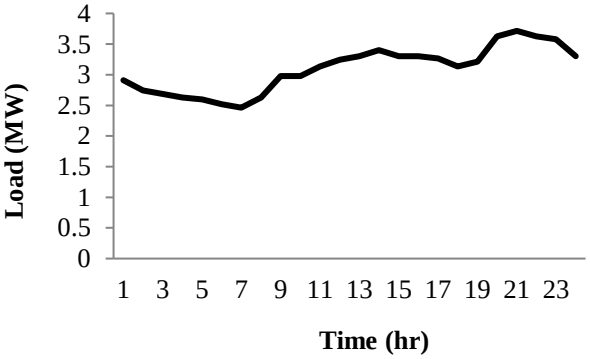

Figure. 3 Typical daily load curve of modified IEEE-33 EDN as defined in Ref. [33]

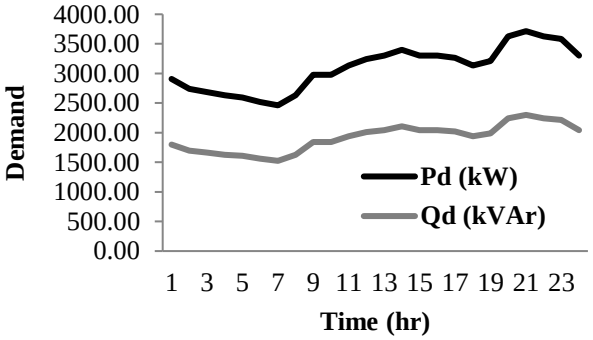

Figure. 4 Active and reactive power load profile for constant power load model

The bus voltage magnitudes are set to optimize between 0.95 to 1.05 p.u., and the OLTC and PST controls at substation (i.e., in branch 1) are not taken in to account. With these modifications, the NR load flow is performed to determine the net effective loading profile of MG for each hour. Then, OPF using AGOA are performed. In OPF, AGOA needs optimize 12 control variables, which include five generators active output powers, five generators voltage magnitudes (and correspondingly reactive output powers), two CB/D-STATCOM reactive power injections. Simulations are performed in two cases and presented below.

5.1.1. OPF in radial MG

In this Case 1, the switchable tie-lines are remained open and thus MG maintained basic radial configuration. The loads are considered as constant power load model. The daily active and reactive load profile for this load model is given in Fig. 4.

The results of OPF for 24-hours are given in Table 1. Total operating cost (f_1) in \$/hr, real power losses (f_2) in kW, average voltage deviation index (f_3), overall voltage stability index (f_4) are provided in respective columns. For the peak-hour (i.e., 8-9pm), the AGOA optimized controlling parameters in OPF problem (i.e., the generators' active power outputs in kW, reactive power generations in kVAr, and generator bus voltages in p.u.) are given in Table 2.

Similarly, the controlling parameters when network has experienced better performance (i.e., 9-10am) are given in Table 3. Though the maximum SPV penetration is occurred at 12:1pm, the better performance is observed at 9-10am. This indicates the need of either RE curtailment (since SPV DGs are not dispatchable sources) or energy storage, which is another important aspect to be considered for more efficient operation of MG.

Table 1. Optimal results of AGOA for Case 1 and Case 2

Hr	Case 1				Case2			
	F_1	F_2	F_3	F_4	F_1	F_2	F_3	F_4
12-1am	1115.92	82.0776	0.0058	0.7872	1114.563	50.041	0.0023	0.8364
1-2	1113.78	72.3651	0.0052	0.7996	1112.592	44.526	0.0021	0.8456
2-3	1113.09	69.3498	0.0050	0.8037	1111.937	42.784	0.0020	0.8486
3-4	1112.38	66.3607	0.0049	0.8078	1111.279	41.060	0.0020	0.8516
4-5	1111.95	64.5848	0.0048	0.8103	1110.882	40.033	0.0019	0.8534
5-6	1110.96	60.6183	0.0045	0.8160	1109.962	37.706	0.0018	0.8577
6-7	1110.26	57.8597	0.0044	0.8201	1109.294	36.062	0.0018	0.8608
7-8	1111.98	58.2150	0.0044	0.8212	1108.904	30.623	0.0015	0.8725
8-9	1115.76	64.1445	0.0047	0.8146	1109.436	26.746	0.0012	0.8816
9-10	1115.35	56.2692	0.0042	0.8266	1106.968	20.211	0.0008	0.8971
10-11	1117.07	59.2748	0.0045	0.8225	1107.201	20.042	0.0011	0.8974
11-Noon	1118.35	62.5612	0.0046	0.8178	1107.707	20.678	0.0013	0.8957
12-1pm	1119.02	64.8069	0.0048	0.8147	1108.131	21.292	0.0013	0.8942
1-2	1120.40	72.4223	0.0052	0.8045	1109.924	24.261	0.0012	0.8872
2-3	1119.35	71.1828	0.0051	0.8059	1110.074	25.134	0.0010	0.8854
3-4	1119.69	78.4295	0.0056	0.7961	1112.106	30.968	0.0013	0.8729
4-5	1119.74	86.8694	0.0061	0.7845	1114.450	40.429	0.0018	0.8544
5-6	1118.51	89.6189	0.0063	0.7794	1115.627	49.227	0.0022	0.8385
6-7	1119.78	101.4949	0.0069	0.7646	1118.111	60.632	0.0026	0.8203
7-8	1125.13	132.3496	0.0085	0.7330	1122.958	76.824	0.0032	0.7983
8-9	1126.30	139.7067	0.0089	0.7261	1124.010	80.570	0.0033	0.7935
9-10	1125.13	132.3496	0.0085	0.7330	1122.958	76.824	0.0032	0.7983
10-11	1124.56	128.8399	0.0083	0.7364	1122.448	75.042	0.0031	0.8006
11-12pm	1120.94	107.7751	0.0072	0.7578	1119.165	63.977	0.0027	0.8155

*F_1 in \$/hr, F_2 in kW, F_3 and F_4 in p.u.

Table 2. Optimized parameters for Case 1 during 8-9pm and 9-10am

At peak-hour (8-9pm)					At optimal SPV penetration level (9-10am)				
PG_1	PG_{18}	PG_{22}	PG_{25}	PG_{33}	PG_1	PG_{18}	PG_{22}	PG_{25}	PG_{33}
3854.707	0	0	0	0	2425.896	151.595	151.592	151.593	151.594
QG_1	QG_{18}	QG_{22}	QG_{25}	QG_{33}	QG_1	QG_{18}	QG_{22}	QG_{25}	QG_{33}
1422.931	374.197	0	0	599.062	1003.210	278.514	0	0	599.752
V_1	V_{18}	V_{22}	V_{25}	V_{33}	V_1	V_{18}	V_{22}	V_{25}	V_{33}
1.0499	0.9892	1.0422	1.0228	0.9954	1.0499	1.0162	1.0467	1.0324	1.0198

*PG in kW, QG is kVAr, V in p.u.

Table 3. Optimized parameters for Case 2 during 8-9pm and 10-11am

At peak-hour (8-9pm)					At optimal SPV penetration level (10-11am)				
PG_1	PG_{18}	PG_{22}	PG_{25}	PG_{33}	PG_1	PG_{18}	PG_{22}	PG_{25}	PG_{33}
3664.170	0	0	0	0	1647.063	181	181	181	181
QG_1	QG_{18}	QG_{22}	QG_{25}	QG_{33}	QG_1	QG_{18}	QG_{22}	QG_{25}	QG_{33}
1001.120	4.247	0	0	214.235	840.378	0.000	0	0	180.218
V_1	V_{18}	V_{22}	V_{25}	V_{33}	V_1	V_{18}	V_{22}	V_{25}	V_{33}
1.0498	1.0245	1.0303	1.0227	1.0236	1.0472	1.0498	1.0410	1.0342	1.0400

*PG in kW, QG is kVAr, V in p.u.

Table 7. Comparison of AGOA based OPF results in IEEE 30-bus

Method	F_1 ($/hr)	F_2 (MW)	Method	F_1 ($/hr)	F_2 (MW)
PSO [13]	828.132	8.350	DEA [16]	799.083	8.630
MOO [15]	822.430	5.687	BSA [19]	799.076	8.654
MVO [13]	810.901	7.680	PSOGSA [17]	799.071	8.625
GOA [13]	809.741	10.090	ICBO [21]	799.035	8.613
HHO [13]	804.141	7.970	ICEFO [22]	799.034	8.615
SF-DE [18]	800.413	9.010	MFO [20]	798.945	-
MOALO [12]	799.144	8.640	WOA [11]	798.028	7.754
CSA [14]	799.129	8.654	WOA-WM [11]	797.667	8.426
HCSA-SFO [14]	799.118	8.646	**AGOA**	**789.034**	**8.615**

5.1.2. OPF in meshed MG

In this Case 2, the switchable tie-lines are closed and thus MG converted into meshed network. The loads are modelled as proposed composite load. In similar to Case 1, the optimized objective functions for Case 2 are given in Table 1. Similarly, the controlling parameters when network has experienced better performance (i.e., 10-11am) are given in Table 3. Though the maximum SPV penetration is occurred at 12:1pm, the better performance is observed at 9-10am. Also, the AGOA optimized controlling parameters in OPF are given for peak-hour and Table 6.

In comparison to Case 1, improved network performance is observed in all the aspects in Case 2. Among all objectives, loss is critical in EDN operation, the comparison between radial and meshed network can be observed in Fig. 6. From these, it can be observed that the overall performance of the MG enhanced not only technical point of view but also economically irrespective of the level of variability.

5.2 OPF in conventional power system

According to [11-22], an IEEE 30-bus power system with 41 transmission lines has been widely explored, and the same is taken into account here for comparison and validation of the suggested AGOA's efficiency. It features a total of 25 control variables (e.g., 6 generators' real power adjustments and voltage magnitudes, 4 tap-changers, and 9 shunt VAr controls) and is optimised for lowering fuel costs.

Table 7 summarises AGOA's findings and compares them to other literature. This comparison demonstrates the proposed method's efficacy and robustness, and we can conclude that the AGOA algorithm produces very competitive outcomes when compared with other methods.

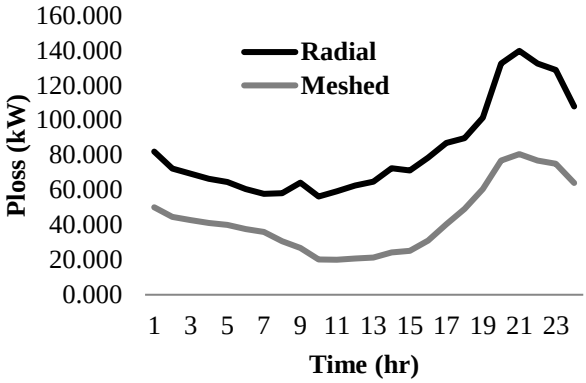

Figure. 6 Comparison of active power loss for radial and meshed configuration

6. Conclusion

In this paper, OPF problem in MG considering variability in photovoltaic power generation and network loading profile is presented. To resemble realistic loading effect, residential, industrial, commercial, electric vehicles and agricultural loads are taken into account. The complexity involved in OPF problem with various multi-objectives, operational equal and unequal constraints is solved using an efficient meta-heuristic grasshopper optimization algorithm (AGOA) with adaptive controlling parameter for balancing between exploitation and exploration phases in the optimization process. Simulations are performed in modified IEEE 33-bus MG over 24-hour span. The algorithm is successful in providing feasible and optimal values at each scheduling hour with low operational cost, reduced distribution losses, good voltage profile and high voltage stability margin. And, the switching between radial to meshed network results of overall improved performance irrespective of variability in the network.

Conflicts of interest

The authors declare no conflict of interest.

Author contributions

P Sobha Rani: Conceptualization and writing-original draft preparation. M.S. Giridhar: Writing-original draft preparation and formal analysis. N K Radha Rani: Writing-review and editing. Varaprasad Janamala: Conceptualization, methodology, software simulation and results validation.

References

[1] B. F. Wollenberg and A. J. Wood, *Power System Generation Operation and Control*, Willey & Sons, New York, 1996.

[2] N. P. Padhy, "Unit commitment-a bibliographical survey", *IEEE Transactions on Power Systems*, Vol. 19, No. 2, pp. 1196-1205, 2004.

[3] Y. F. Li, N. Pedroni, and E. Zio, "A memetic evolutionary multi-objective optimization method for environmental power unit commitment", *IEEE Transactions on Power Systems*, Vol. 28, No. 3, pp. 2660-2669, 2013.

[4] J. M. L. Rojas, G. J. Osório, and J. P. Catalão, "New probabilistic method for solving economic dispatch and unit commitment problems incorporating uncertainty due to renewable energy integration", *International Journal of Electrical Power & Energy Systems*, Vol. 78, pp. 61-71, 2016.

[5] S. Frank, I. Steponavice, and S. Rebennack, "Optimal power flow: a bibliographic survey I", *Energy Systems*, Vol. 3, No. 3, pp. 221-258, 2012.

[6] S. Frank, I. Steponavice, and S. Rebennack, "Optimal power flow: a bibliographic survey II", *Energy Systems*, Vol. 3, No. 3, pp. 259-289, 2012.

[7] M. A. A. Moamen and N. P. Padhy, "Optimal power flow incorporating FACTS devices-bibliography and survey", In: *Proc. of 2003 IEEE PES Transmission and Distribution Conference and Exposition*, Dallas, TX, USA, 2003.

[8] P. Siano, "Demand response and smart grids-A survey", *Renewable and Sustainable Energy Reviews*, Vol. 30, pp. 461-478, 2014.

[9] E. Mohagheghi, M. Alramlawi, A. Gabash, and P. Li, "A survey of real-time optimal power flow", *Energies*, Vol. 11, No. 11, p. 314, 2018.

[10] M. Ebeed, S. Kamel, and F. Jurado, "Optimal power flow using recent optimization techniques", *Classical and Recent Aspects of Power System Optimization*, pp. 157-183. Academic Press, 2018.

[11] V. Mukherjee, A. Mukherjee, and D. Prasad, "Whale optimization algorithm with wavelet mutation for the solution of optimal power flow problem", *Handbook of Research on Predictive Modeling and Optimization Methods in Science and Engineering*, pp. 500-553, 2018.

[12] O. Herbadji, L. Slimani, and T. Bouktir, "Optimal power flow with four conflicting objective functions using multiobjective ant lion algorithm: A case study of the algerian electrical network", *Iranian Journal of Electrical and Electronic Engineering*, Vol. 15, No. 1, pp. 94-113, 2019.

[13] H. Diab, M. Abdelsalam, and A. Abdelbary, "A Multi-Objective Optimal Power Flow Control of Electrical Transmission Networks Using Intelligent Meta-Heuristic Optimization Techniques", *Sustainability*, Vol. 13, No. 9, 4979, 2021.

[14] T. L. Duong, N. A. Nguyen, and T. T. Nguyen, "A Newly Hybrid Method Based on Cuckoo Search and Sunflower Optimization for Optimal Power Flow Problem", *Sustainability*, Vol. 12, No. 13, 5283, 2020.

[15] S. S. Reddy, "Solution of multi-objective optimal power flow using efficient meta-heuristic algorithm", *Electrical Engineering*, Vol. 100, No. 2, pp. 401-413, 2018.

[16] A. M. Shaheen, R. A. E. Sehiemy, and S. M. Farrag, "Optimal Power Flow using Forced Initialized Multi-Objective Differential Evolution Algorithm," In: *Proc. of 17th International Middle East Power Systems Conference*, Mansoura University, Egypt, 2015.

[17] J. Radosavljević, D. Klimenta, M. Jevtić, and N. Arsić, "Optimal power flow using a hybrid optimization algorithm of particle swarm optimization and gravitational search algorithm", *Electric Power Components and Systems*, Vol. 43, No. 17, pp. 1958-1970, 2015.

[18] P. P. Biswas, P. N. Suganthan, R. Mallipeddi, and G. A. Amaratunga, "Optimal power flow solutions using differential evolution algorithm integrated with effective constraint handling techniques", *Engineering Applications of Artificial Intelligence*, Vol. 68, pp. 81-100, 2018.

[19] A. E. Chaib, H. R. Bouchekara, R. Mehasni, and M. A. Abido, "Optimal power flow with emission and non-smooth cost functions using backtracking search optimization algorithm", *International Journal of Electrical Power & Energy Systems*, Vol. 81, pp. 64-77, 2016.

[20] B. Bentouati, L. Chaib, and S. Chettih. "Optimal power flow using the moth flam optimizer: A case study of the Algerian power system", *Indonesian Journal of Electrical Engineering and Computer Science*, Vol. 1, No. 3, pp. 431-445, 2016.

[21] H. R. Bouchekara, A. E. Chaib, M. A. Abido, and R. A. E. Sehiemy, "Optimal power flow using an Improved Colliding Bodies Optimization algorithm", *Applied Soft Computing*, Vol. 42, pp. 119-131, 2016.

[22] H. Bouchekara, "Solution of the optimal power flow problem considering security constraints using an improved chaotic electromagnetic field optimization algorithm", *Neural Computing and Applications*, Vol. 32, No. 7, pp. 2683-2703, 2020.

[23] S. P. Adam, S. A. Alexandropoulos, P. M. Pardalos, and M. N. Vrahatis, "No free lunch theorem: A review", *Approximation and Optimization*, Vol. 145, pp. 57-82, 2019.

[24] S. Saremi, S. Mirjalili, and A. Lewis, "Grasshopper optimisation algorithm: theory and application", *Advances in Engineering Software*, Vol. 105, pp. 30-47, 2017.

[25] L. Abualigah, and A. Diabat, "A comprehensive survey of the Grasshopper optimization algorithm: results, variants, and applications", *Neural Computing and Applications*, Vol. 32, pp. 15533–15556, 2020.

[26] Y. Meraihi, A. B. Gabis, S. Mirjalili, and A. R. Cherif, "Grasshopper optimization algorithm: theory, variants, and applications", *IEEE Access*, Vol. 9, pp. 50001-50024, 2021.

[27] J. Liu, A. Wang, Y. Qu, and W. Wang, "Coordinated operation of multi-integrated energy system based on linear weighted sum and grasshopper optimization algorithm", *IEEE Access*, Vol. 6, pp. 42186-42195, 2018.

[28] P. P. Biswas, P. N. Suganthan, and G. A. Amaratunga, "Optimal power flow solutions incorporating stochastic wind and solar power", *Energy Conversion and Management*, Vol. 148, pp. 1194-1207, 2017.

[29] N. Taleb, B. Bentouati, and S. Chettih, "Optimal power flow solutions incorporating stochastic solar power with the application grey wolf optimize", *Algerian Journal of Renewable Energy and Sustainable Development*, Vol. 3, No. 1, pp. 74-84, 2021.

[30] M. A. Shaheen, H. M. Hasanien, S. F. Mekhamer, and H. E. Talaat, "Optimal power flow of power systems including distributed generation units using sunflower optimization algorithm", *IEEE Access*, Vol. 7, pp. 109289-109300, 2019.

[31] C. Shilaja and K. Ravi, "Optimal power flow using hybrid DA-APSO algorithm in renewable energy resources", *Energy Procedia*, Vol. 117, pp. 1085-1092, 2017.

[32] K. V. Kavuturu and P. V. Narasimham, "Transmission Security Enhancement under (N− 1) Contingency Conditions with Optimal Unified Power Flow Controller and Renewable Energy Sources Generation", *Journal of Electrical Engineering & Technology*, Vol. 15, No. 4, pp. 1617-1630, 2020.

[33] S. H. Dolatabadi, M. Ghorbanian, P. Siano, and N. D. Hatziargyriou, "An Enhanced IEEE 33 Bus Benchmark Test System for Distribution System Studies", *IEEE Transactions on Power Systems*, Vol. 36, No. 3, pp. 2565-2572, 2020.

[34] V. Janamala and T. K. Pandraju, "Static voltage stability of reconfigurable radial distribution system considering voltage dependent load models", *Mathematical Modelling of Engineering Problems*, Vol. 7, No. 3, pp. 450-458, 2020.

[35] J. Liu, A. Wang, Y. Qu, and Wang, "Coordinated operation of multi-integrated energy system based on linear weighted sum and grasshopper optimization algorithm", *IEEE Access*, Vol. 6, pp. 42186-42195, 2018.